J Seismol (2008) 12:35–51
DOI 10.1007/s10950-007-9069-8

ORIGINAL ARTICLE

Simulation of accelerograms from simplified deterministic approach for the 23rd October 2004 Niigata-ken Chuetsu, Japan earthquake

A. Joshi · K. Mohan

Received: 7 September 2006 / Accepted: 22 October 2007 / Published online: 29 November 2007

Abstract A simple hybrid approach for the simulation of strong ground motion is presented in this paper. This approach is based on the deterministic modelling of rupture plane initially started by Midorikawa, Tectonophysics 218:287–295, (1993) and further modified by Joshi, Pure Appl Geophys (PAGEOPH) 8:161, (2004). In this technique, the finite rupture plane of the target event is divided into several subfaults, which satisfy scaling relationship. In this paper, simulation of strong ground motion due to a rupture buried in a earth medium consisting of several layers of different velocities and thicknesses is made by considering (1) transmission of energy at each layer; (2) frequency filtering properties of medium and earthquake source; (3) correction factor for slip of large and small magnitude earthquakes and (4) site amplification ratio at various stations. To test the efficacy of the developed technique, strong motion records were simulated at different stations that have recorded the 2004 Niigata-ken Chuetsu, Japan earthquake (M_s 7.0). Comparison is made between the simulated and observed velocity and acceleration records and their response spectra. Distribution of peak ground acceleration, velocity and displacement surrounding the rupture plane is prepared from simulated and observed records and are compared with each other. The comparison of synthetic with the observed records over wide range of frequencies shows that the present technique is effective to predict various strong motion parameters from simple deterministic model which is based on simple regression relations and modelling parameters.

Keywords Deterministic approach · Envelope · Accelerogram · White noise · Amplification factor

A. Joshi (✉)
Department of Earth Sciences,
Indian Institute of Technology Roorkee,
Roorkee 247 667, India
e-mail: anushijos@yahoo.co.in

K. Mohan
Institute of Seismological Research,
Gandhinagar 382018, Gujarat, India

1 Introduction

Reliable prediction of strong ground motion plays significant role for the construction of earthquake resistant design in any seismically active region. A number of techniques have been proposed to simulate strong ground motion. Among these are (1) composite source modelling technique (Zeng et al. 1994; Yu 1994; Yu et al. 1995; Saikia and Herrmann 1985; Saikia 1993); (2) stochastic simulation technique (Boore 1983; Boore and Atkinson 1987; Lai 1982) and (3) empirical Greens function technique (Irikura 1986; Hartzell 1978; 1982; Kanamori 1979; Hadley and Helmberger 1980; Mikumo et al. 1981; Irikura and Muramatu 1982; Irikura 1983, 1986; Kamae and

Irikura 1998; Mugnuia and Brune 1984; Hutchings 1985). In the composite source modelling, technique synthetic accelerograms are simulated by modelling the earthquake source process and the propagation of energy in the medium. This technique requires a detailed velocity Q structure of the region, the fault plane solution and the stress drop parameters. One of the most difficult parts of this simulation technique is the selection of these parameters at the site of interest. The stochastic simulation technique is based on the theoretical spectrum defined by simple seismological model of source and propagation filters. However, this technique lacks complete representation of finite rupture source. The empirical Green function (EGF) technique requires the records of small events at those stations at which simulation is desired. However, the records of small events, which mainly consist of foreshocks or aftershocks from the source region of the target earthquake, are not easily available at all sites of interest. Therefore, the estimation of the strong motion parameters using EGF techniques is a difficult task, especially in those regions where we have limited information in hand. Kamae and Irikura (1992) have presented a technique in which records of small events used in the EGF technique are replaced by stochastically simulated ground motion based on seismological spectral model. This method lacks the use of shaping time window based on kinematic source model of rupture plane. Midorikawa (1993) proposed a technique that is based on the EGF technique of Irikura (1986). This technique uses the envelope of acceleration records in place of small events used in the EGF technique. Although this technique is useful for predicting important ground motion parameters like peak ground acceleration and duration, it lacks complete characterisation of strong ground motion in terms of frequency characteristics. This limitation has been removed by Joshi et al. (2001) by incorporating the stochastic nature of the strong ground motion and using envelope function based on kinematic model of rupture plane as shaping time window. Modification in this technique has been made by Joshi and Midorikawa (2004) by placing the rupture in a layered earth model and considering the correction for slip duration of small and large earthquakes. This modified technique is tested with the strong motion data of Himalayan and Japanese earthquakes (Joshi 2004; Joshi and Midorikawa 2004, 2005).

Although these refinements gives reliable simulations in a wide frequency range, the component-wise simulation of strong motion records is needed for reliable assessment of engineering parameters. The work presented in this paper is the modification of the above technique to simulate the component of the strong motion records using the site amplification ratios at various sites.

2 Methodology

The technique presented in this paper is based on semi-empirical method proposed by Midorikawa (1993) and later modified by Joshi (1997), Joshi et al. (2001) and Joshi and Midorikawa (2005). In this method, the entire rupture plane is divided into several small rupture planes which are termed as elements or subfaults. The basis of the division is self-similarity laws given by Kanamori and Anderson (1975). These laws are discussed in detail by Joshi (2004). The entire scheme of semi-empirical simulation is similar to the EGF technique except in the use of empirical function in place of small events. In this semi-empirical method, we use the envelope function, which is mathematically given as (Joshi et al. 2001):

$$e(t) = T_{ss}\left(\frac{a(g)t}{T_d}\right)e^{1-\left(\frac{t}{T_d}\right)} \quad (1)$$

Parameters $a(g)$ and T_d are the peak ground acceleration and duration parameters, respectively. Their choice had been carefully made from regression relations after testing their applicability in the influential area of the target earthquake. The parameter T_{ss} is the transmission coefficient of the incidented shear wave. The transmission coefficient of the incidented S wave in a solid layer given by Joshi et al. (2001) and Joshi and Midorikawa (2004) for modelling the effect of the transmission of the energy in a layered earth has been used in this work.

First subfault to release energy is the nucleation point. Other subfaults release energy when rupture reaches their center following the geometry of rupture propagation. In the present work, radial rupture geometry has been assumed. For a multi-layered earth model, the travel time of the energy from the subfault to the observation point is calculated by tracing the ray from each subfault within the rupture plane to the

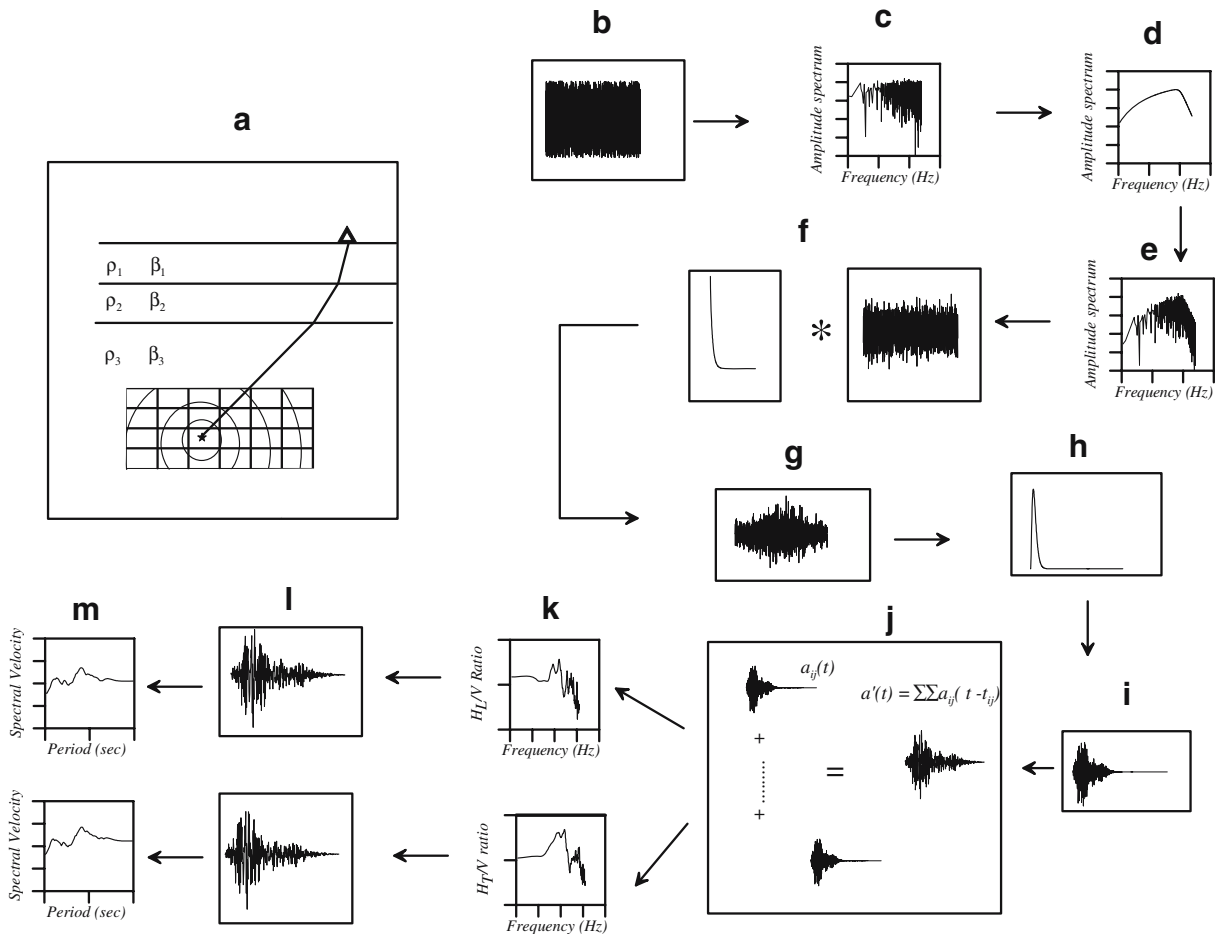

Fig. 1 **a** Rupture model in a layered earth medium. Radial rupture geometry is assumed. *Star* denotes nucleation point. **b** White Gaussian noise and its spectrum at **c**. **d** The theoretical spectrum of acceleration record. **e** Multiplication of spectrum of acceleration record with the spectrum of white noise. **f** The filtered sequence and its convolution with the correction function. **g** Obtained sequence after convolution with the correction function. **h** Shaping window used for making random sequence into finite sequence. **i** Obtained vertical component of record after windowing. **j** Summation of records from each element to simulate the vertical component of acceleration record of the target earthquake. **k** Site amplification curve (*H*/*V*) obtained from the longitudinal and transverse component of observed acceleration records. **l** The simulated transverse and longitudinal components of the records after filtering it with the site amplification curve. **m** The response curve at 5% damping

observation point using the method given by Lee and Stewart (1981). Brief discussion of this method is given by Joshi et al. (2001) and Joshi and Midorikawa (2004). The total time travelled by seismic energy at the observation point depends on the time taken by rupture propagation from the nucleation point to a particular subfault and the travel time of energy in the layered earth from that subfault to the observation point.

For simulation of time series having basic spectral properties of acceleration record, we have used the modified form of stochastic simulation

Table 1 Parameter of the 2004 Niigata-ken Chuetsu earthquake, Japan

Hypocenter	Size source	Fault plane solution	Ref.
8:56:4.8(GMT)	m_b=6.4,	NP1: φ=23,	CMT
37.31N, 138.83E	M_s=7.0	δ=39, λ=86	
13 km	M_o=8.6×10^{25} dyne-cm	NP2:φ=209, δ=51, λ=93	(Harvard)
	M_W=6.6		
	m_s=6.3		
	M_{JMA}=6.8		

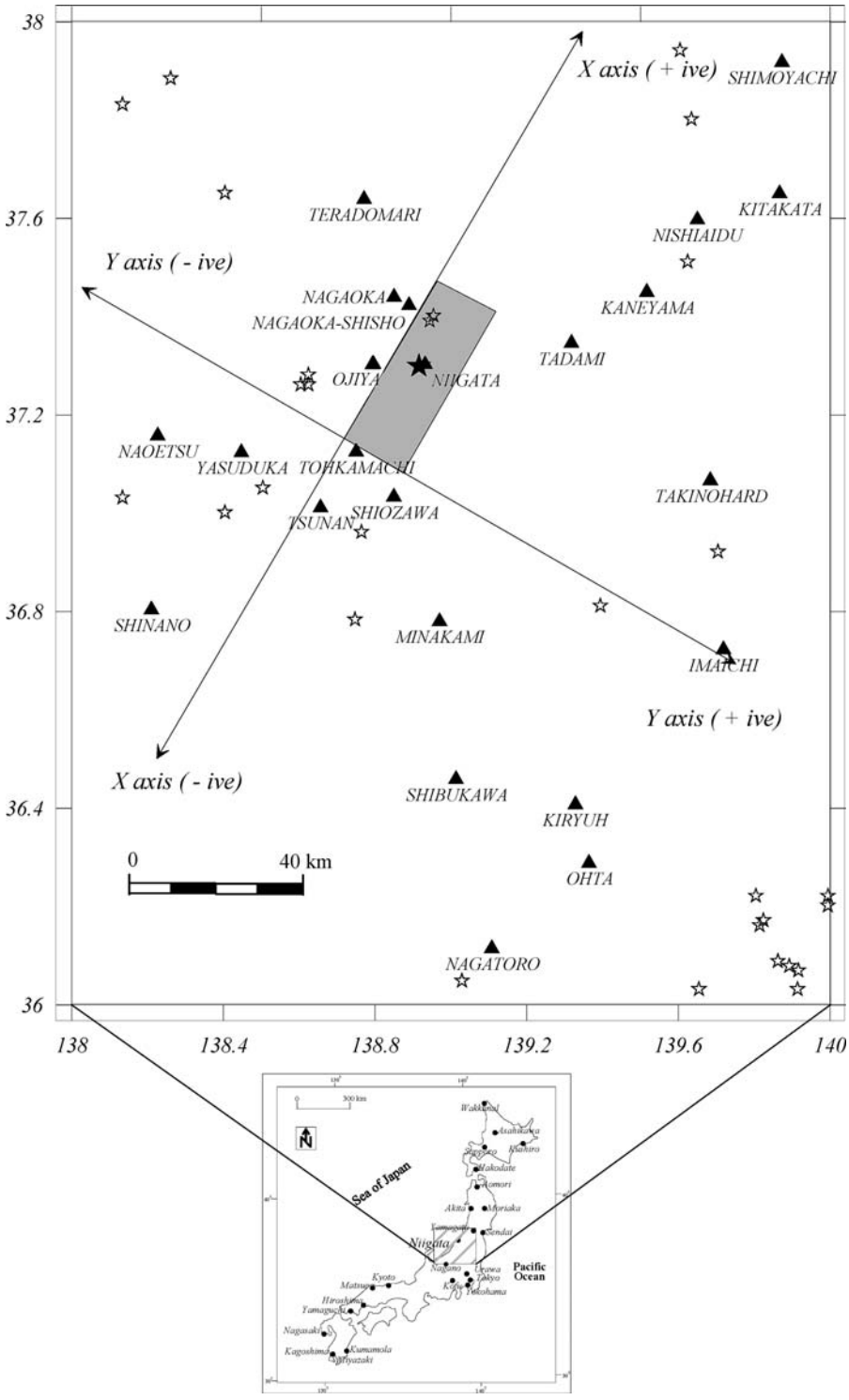

Fig. 2 Location of rupture responsible for the 2004 Niigata-ken Chuetsu earthquake, Japan. The source region is shown by *shaded region*. Location of some of the stations of strong motion network at which simulation is made is shown by *solid triangles* (modified after http://www.k-net.bosai.go.jp/k-net). Location of events that are used for site amplification study at various station is shown by *open star*

technique given by Boore (1983). In this modified form, the envelope of accelerogram released by subfaults has been used as the shaping window. The stochastic simulation technique uses white Gaussian noise with zero expected mean and the variance chosen to give unit spectral amplitude on an average. The record having basic spectral shape of accelerogram is obtained after the white Gaussian noise is

Table 2 Detail of site codes of stations used for simulation purpose

Sr. no.	Station code	Latitude	Longitude	Station name
1	NIG022	37.03	138.84	SHIOZAWA
2	NIG021	37.12	138.75	TOHKAMACHI
3	NIG019	37.30	138.79	OJIYA
4	NIG016	37.64	138.77	TERADOMARI
5	NIG028	37.42	138.89	NAGAOKA-SHISHO
6	NIG023	37.01	138.66	TSUNAN
7	NIG024	37.12	138.44	YASUDUKA
8	GNM002	36.78	138.97	MINAKAMI
9	FKS022	37.59	139.65	NISHIAIDU
10	YMT014	37.92	139.87	SHIMOYACHI
11	TCG009	36.72	139.71	IMAICHI
12	SIT004	36.11	139.10	NAGATORO
13	NIG025	37.16	138.22	NAOETSU
14	NIG010	37.30	138.93	NIIGATA
15	NGN002	36.80	138.21	SHINANO
16	GNM013	36.31	139.02	TAKASAKI
17	GNM011	36.29	139.36	OHTA
18	GNM009	36.41	139.33	KIRYUH
19	FKS030	37.45	139.52	KANEYAMA
20	FKS028	37.35	139.32	TADAMI
21	FKS021	37.65	139.86	KITAKATA
22	FKS027	37.07	139.68	TAKINOHARD
23	GNM007	36.46	139.01	SHIBUKAWA

The location of stations and their names are reproduced from K-net site (http://www.k-net.bosai.go.jp/k-net).

passed through number of filters representing the earthquake processes. The observed acceleration spectra at particular station at distance 'R' is given as (Boore 1983):

$$A(f)=S(f)P(\mathrm{f})F_1(f,R) \tag{2}$$

The filter $S(f)$ in Eq. 2 represents the source spectrum, which follows omega-square decay of high frequencies as defined by Brune (1970), the filter $P(f)$ represents near site attenuation of high frequencies. The filter $F_1(f, R)$ in Eq. 2 represents the effect of anelastic attenuation. When white Gaussian noise is passed through above filters, a record having spectral shape of accelerogram is obtained. This accelerogram is made finite length sequence by windowing it in time domain. In this work, the envelope of accelerogram given in Eq. 1 is used as window function. Using this approach, the envelope of vertical peak ground acceleration is simulated. Hence, after windowing the filtered record obtained from Eq. 2, the vertical component of accelerogram is simulated.

Site amplification curve plays important role in resolving the generated vertical component into horizontal component. There are two methods from which site amplification curve at various sites can be obtained from the earthquake records after removing the source and propagation effects. First is from horizontal component spectral ratio (H/H ratio) relative to reference site (Seo and Samano 1993). The second is from the spectral ratio of horizontal component relative to vertical component (H/V ratio; Nakamura 1988). The major problem in H/H ratio is whether it coincides with relative site amplifications of seismic shear wave incidence (Horike et al. 2001). Site amplification using single-station recording is easily applied and it directly estimates the site amplification factor without using a reference site; much research has been done to investigate its validity by observation and by theory (Horike et al. 2001). One of major application of H/V ratio method is in the component-wise simulation of high-frequency ground motion using stochastic simulation technique (Boore 1983; Beresnev and Atkinson 1997). In the present work, we have used the NS and EW component of observed records of small events at each station to obtain H/V ratio. The H/V ratio is computed from the portion of record, which contains S-wave phase. At each station, two H/V ratio curves are obtained, i.e. one for NS and other for EW component. The simulated NS and EW component of strong motion records are obtained after multiplying the spectrum of simulated vertical component with these two H/V ratio curves. To compensate the appropriate difference in the slip of large and small earthquake, the simulated record is further convolved with the following correction function '$F(t)$'given by Irikura et al. (1997):

$$F(t)=\delta(t)+\left\{\frac{N-1}{T}\left(1-e^{-1}\right)\right\}e^{-\left(\frac{t}{T}\right)} \tag{3}$$

In this equation, $\delta(t)$ is the delta function, N is the total number of subfaults along the length or the width of rupture plane, and 'T' is the rise time of the target earthquake. We have used the following relation by Somerville et al. (1999) for computing the rise time:

$$T=2.03\times10^{-9}(M_o)^{1/3} \tag{4}$$

The method of simulation used in this paper is shown in Fig. 1.

Table 3 The detail of events used to calculate *H*/*V* ratio

Date	Time	Latitude (°N)	Longitude (°E)	Depth (km)	Magnitude (JMA)
19 03 2000	12:49:00	37.28	138.62	14	4.3
07 04 2000	15:54:00	37.00	138.40	17	4.1
15 04 2000	5:26:00	36.22	139.99	53	3.9
03 06 2000	17:50:00	37.51	139.62	13	3.6
19 08 2000	16:38:00	36.22	139.80	56	3.8
09 09 2000	20:48:00	36.03	139.65	67	4.2
12 10 2000	05:35:00	37.94	139.60	12	4.1
18 10 2000	12:58:00	36.92	139.70	09	4.5
02 01 2001	19:53:00	37.26	138.60	15	4.4
04 01 2001	13:18:00	36.96	138.76	14	5.1
26 03 2001	05:36:00	37.03	138.13	13	3.6
31 03 2001	06:09:00	36.81	139.39	80	4.9
20 07 2001	06:02:00	36.17	139.82	56	4.8
10 12 2001	00:45:00	37.05	138.50	15	3.5
02 02 2002	05:09:00	37.40	138.95	11	4.3
23 12 2002	05:31:00	36.20	139.99	55	4.1
13 03 2003	12:13:00	36.09	139.86	47	4.8
08 04 2003	04:17:00	36.07	139.91	47	4.6
06 05 2003	23:48:00	36.03	139.91	46	4.3
12 05 2003	0:57:00	35.87	140.09	47	5.2
26 05 2003	18:24:00	38.81	141.68	71	7.0
31 05 2003	2:47:00	36.16	139.81	55	4.0
16 06 2003	18:34:00	36.84	141.27	77	5.0
26 08 2003	09:31:00	37.26	138.62	11	3.8
30 09 2003	12:23:00	37.83	138.13	19	4.3
15 10 2003	16:30:00	35.61	140.05	74	5.1
16 12 2003	19:48:00	36.78	138.74	40	4.2
19 12 2003	12:49:00	38.14	137.94	27	4.4
22 12 2003	21:07:00	37.88	138.26	16	4.7
23 01 2004	18:01:00	37.26	141.13	66	5.3
07 03 2004	03:41:00	36.05	139.03	09	3.4
15 03 2004	07:38:00	37.65	138.40	24	4.7
04 04 2004	08:02:00	36.39	141.16	49	5.8
10 06 2004	23:40:00	35.99	140.09	66	5.7
10 07 2004	20:07:00	36.08	139.89	48	4.7
04 08 2004	04:17:00	36.44	140.62	58	4.9
07 09 2004	21:41:00	37.39	138.94	00	4.3
21 09 2004	06:11:00	37.80	139.63	20	3.7

The location and other given information of these events is reproduced from K-net site (http://www.k-net.bosai.go.jp/k-net).

3 Data set

On the 23rd of October 2004 at 17:56 (JST), an earthquake (M_{JMA} 6.8; Japan Meteorological Agency) struck mid Niigata prefecture, at 80 km south of Niigata city, on the West coast of Honshu, Japan (Bardet 2004). The parameters of this earthquake are listed in Table 1. Kyoshin Net (K-NET) is a system which sends strong-motion data on the Internet. These data are obtained from 1,000 observatories deployed all over Japan. This system is maintained by National Research Institute for Earth Science and Disaster Prevention (NIED), Japan. The average station-to-station distance is about 25 km. Each station has a digital strong-motion seismograph with a wide frequency band and wide dynamic range having a maximum measurable acceleration of 2,000 gal. The records obtained from these stations are acquired at a

control center in Tsukuba by telemetry. The earthquake of 23rd October 2004 was recorded at 327 stations of Kyoshin network (K-NET) and 286 stations of KiK network (KiK-NET). The data used in this work are downloaded from the K-NET site maintained by NIED, Japan.

In the present method of simulation, we use the site amplification curves at each station. The objectives of using site amplification curve are (1) to simulate components of strong ground motion at a particular site and (2) to include site effects at each station. For computing site amplification curves, we use the H/V ratio method of Nakamura (1988). One advantage of H/V method is that by using this site amplification, we may be able to convert the simulated vertical components into horizontal components. To have a wide coverage of strong motion data in terms of epicentral distance and azimuthal coverage, we have used 23 stations surrounding the rupture plane. Figure 2 shows the location of 23 stations at which we have performed the simulation. These stations lie at epicentral distances that range from 2 to 132 km. The location of these stations is given in Table 2. To have H/V curves at each of these 23 sites, we have selected at least six past events at each station. These events are shown in Fig. 2. The H/V ratio curve is computed from these events after the identification of S-wave phase. Selection of these events depends on the availability of data and clear S-wave phase in the record. The detail of the selected events is given in Table 3. For simulation purpose, we use the average H/V curve at each station. One of such H/V curve at NIG024 station is shown in Fig. 3.

4 Regression relations in the source region of modelled earthquake

Present method of simulation requires various regression relations. These regression relations need to be checked for their applicability in the source region of the target earthquake. In the present work, the regression relation of Abrahamson and Litehiser (1989) has been used for the modelling of the rupture plane of the 2004 Niigata ken-Chuetsu earthquake. To simulate the vertical component of acceleration records following regression relation between vertical peak ground acceleration, magnitude and hypocentral distance has been used (Abrahamson and Litehiser 1989):

$$\begin{aligned}\mathrm{Log}_{10}\, a(g) = &-1.15 + .245M \\ &- 1.0962\mathrm{Log}_{10}\left(R + \mathrm{e}^{.256M}\right) \\ &+ .096F - .0011ER \end{aligned} \quad (5)$$

In this expression, M is the magnitude of an earthquake, R is the hypocentral distance in kilometre, and $a(g)$ is the vertical peak acceleration in centimetre per second squared. The variable E is a dummy variable and is 1 for interplate events and 0 for intraplate events. The dummy variable F is 1 for reverse or reverse oblique events and 0 otherwise. For Japanese earthquakes, the local conditions favour using value E=0, F=1, and hence, the same are used for calculating the acceleration by this expression.

The second regression relationship used in the present work is of the duration parameter, which has been modified by Joshi (2004) to get a fit with the

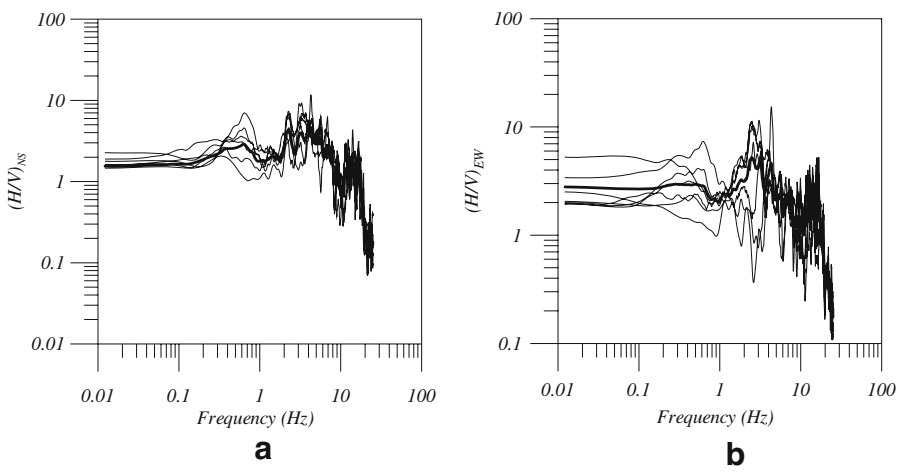

Fig. 3 H/V ratio curve at NIG024 station computed from several events. Prepared H/V ratio curve using **a** NS and **b** EW components

observed data of the Geiyo and Shizuoka earthquakes, Japan (Joshi and Midorikawa 2004, 2005). Using data of the 2004 Niigata ken-Chuetsu earthquake, the duration parameter has been computed at various stations and is shown in Fig. 4. This gives the following modified form of regression relation for duration parameter:

$$T_{\mathrm{d}} = .001510^{.5M} + 1.79R^{0.037} \quad (6)$$

In this expression, M is the magnitude of earthquake, and R is the hypocentral distance in kilometre. Other than these regression relations, the proposed technique requires frequency-dependent Q relations for simulating acceleration records at each site. In the present work, we have used the $Q(f)$ relation given by Kiyono (1992), as it is an average relation for Japan and has been already tested by Joshi and Midorikawa (2004) for simulation of strong ground motion of the Geiyo earthquake of 2001, Japan.

5 Directivity effects

It is seen that strong ground motion usually follows directivity effects. Due to this property peak ground acceleration in the direction of rupture, propagation is higher than in the opposite direction. To test this property, we have made several simulations along the strike direction of the rupture plane. We have selected seven observation points at an interval of 10 km in both sides of the rupture plane. A vertical rupture plane of length 42 km and downward extension 24 km is assumed in this numerical experiment. The dimension of this rupture plane is assumed to be similar to that of the 2004 Niigata-ken Chuetsue earthquake. This rupture plane is divided into 15 elements, each of which corresponds to magnitude 4.7 earthquake and is placed in a layered velocity model. The velocity model used for this case is the same as used for modelling the 2004 Niigata-ken Chuetsu earthquake and is taken after Honda et al. (2004). This model is based on the rupture model assumed by Honda et al. (2004) for estimation of source parameters of this earthquake and is given in Table 4. To have component-wise simulation, we have restricted our numerical experiment with the site effect of station NIG024. Both bilateral and unilateral rupture propagations have been modelled in the numerical experiment and are shown in Fig. 3.

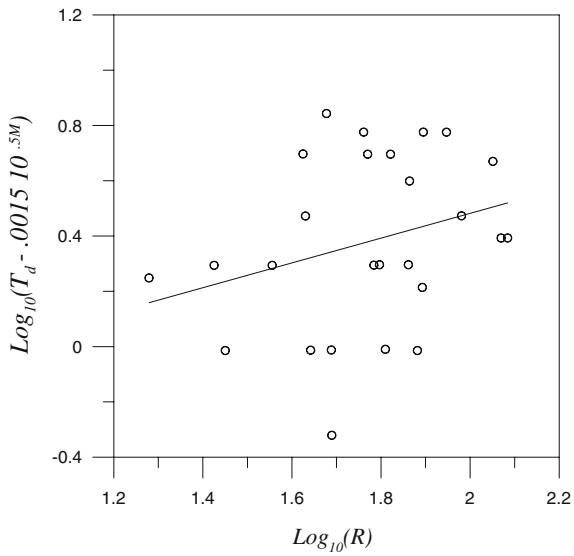

Fig. 4 Plot showing variation of duration parameter with respect to distance

Table 4 Velocity model (after Honda et al. 2004)

Thickness (km)	S Wave velocity (km/s)
7.4	1.9
4.4	3.1
1.4	3.6

It is seen that absolute symmetry is observed in the attenuation curves obtained from NS and EW components for bilateral rupture propagation. This is shown in Fig. 5. In the case of unilateral rupture propagation, peak ground acceleration values in NS and EW components are higher in the direction of rupture propagation compared to peak ground accelerations in the opposite direction of rupture propagation shown in Fig. 5. The simulated records also show an increase in duration of records in the direction opposite to rupture propagation with characteristic decay in peak ground acceleration.

Fig. 5 Attenuation curve for the case of bilateral rupture propagation prepared from simulated NS component shown at **e** and **g**, and EW component shown at **f** and **h**. NS and EW components of accelerogram at two of the near field stations shown in **b** and **d**, respectively. Attenuation curve for the case of unilateral rupture propagation prepared from simulated NS (**m**, **o**) and EW (**n**, **p**) components of accelerogram. NS and EW components of accelerogram at two of the near field stations located in figure is shown in **j** and **l**, respectively

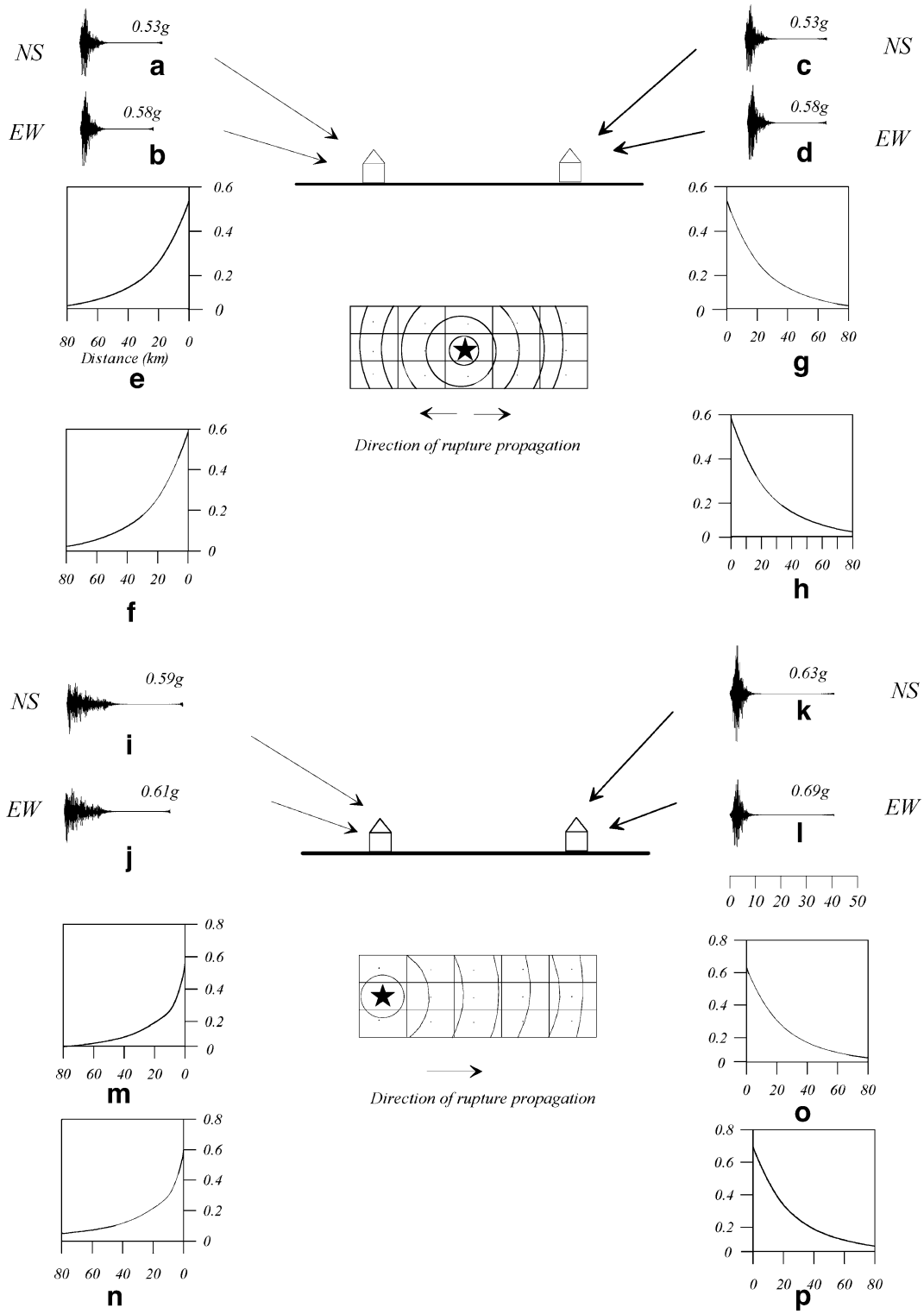
NS
0.53g
a
EW
0.58g
b
0.53g
c
NS
0.58g
d
EW
0.6
0.4
0.2
0
80 60 40 20 0
Distance (km)
e
0 20 40 60 80
g
f
h
Direction of rupture propagation
NS
0.59g
i
EW
0.61g
j
0.63g
k
NS
0.69g
l
EW
0 10 20 30 40 50
0.8
m
n
o
p
Direction of rupture propagation

6 Case study: 2004 Niigata-ken Chuetsu earthquake

The epicentral area of the 2004 Niigata-ken Chuetsu earthquake consists of Neogenic and Quaternary deposits and is shown in Fig. 6. These Neogenic and Quaternary deposits overlay the pyroclastic volcanic basement rocks. The Quaternary deposits generally consist of clay, silt, sand and gravel. The Neogenic formations are heavily folded, and their

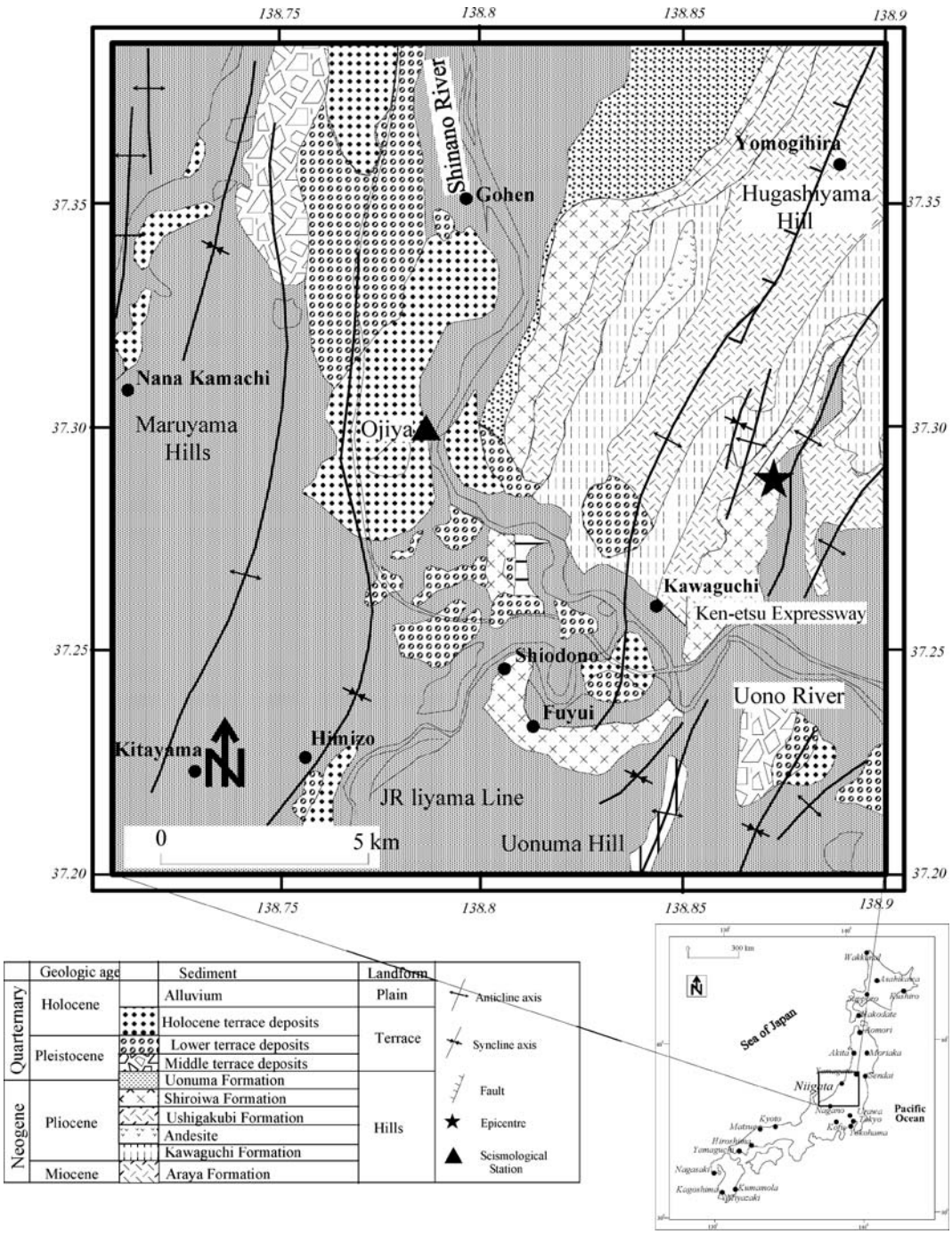

Fig. 6 Geology around the epicentral region of the 2004 Niigata-ken Chuetsu earthquake (modified after Sato et al. 2001)

Table 5 Parameters of rupture model of the 2004 Niigata-ken Chuetsu earthquake, Japan

Modelling parameter
Rupture length=42 km
Width=24 km
Dip=52°
Strike=211°
L_e=4, W_e=3, V_r=3.1 km/s

The parameters L_e, W_e and V_r denote length of elements along length, along downward extension and rupture velocity, respectively.

anticline and syncline axes are aligned NE–SW. The Shinano River flows through the syncline axis, and Tokamachi, Ojiya and Nagaoka are situated in the Shinano valley. Another syncline, which has similar trends, is in the east, and Sumon, Koide, Yamato and Muikamachi towns are located on this syncline along which Uono Stream of Shinano River flows. The anticline and synclines axes are tilted to NE. Uono stream changes its flow direction from NE to NW at Koide town and joins Shinano River nearby Kawaguchi town. This segment of the stream seems to

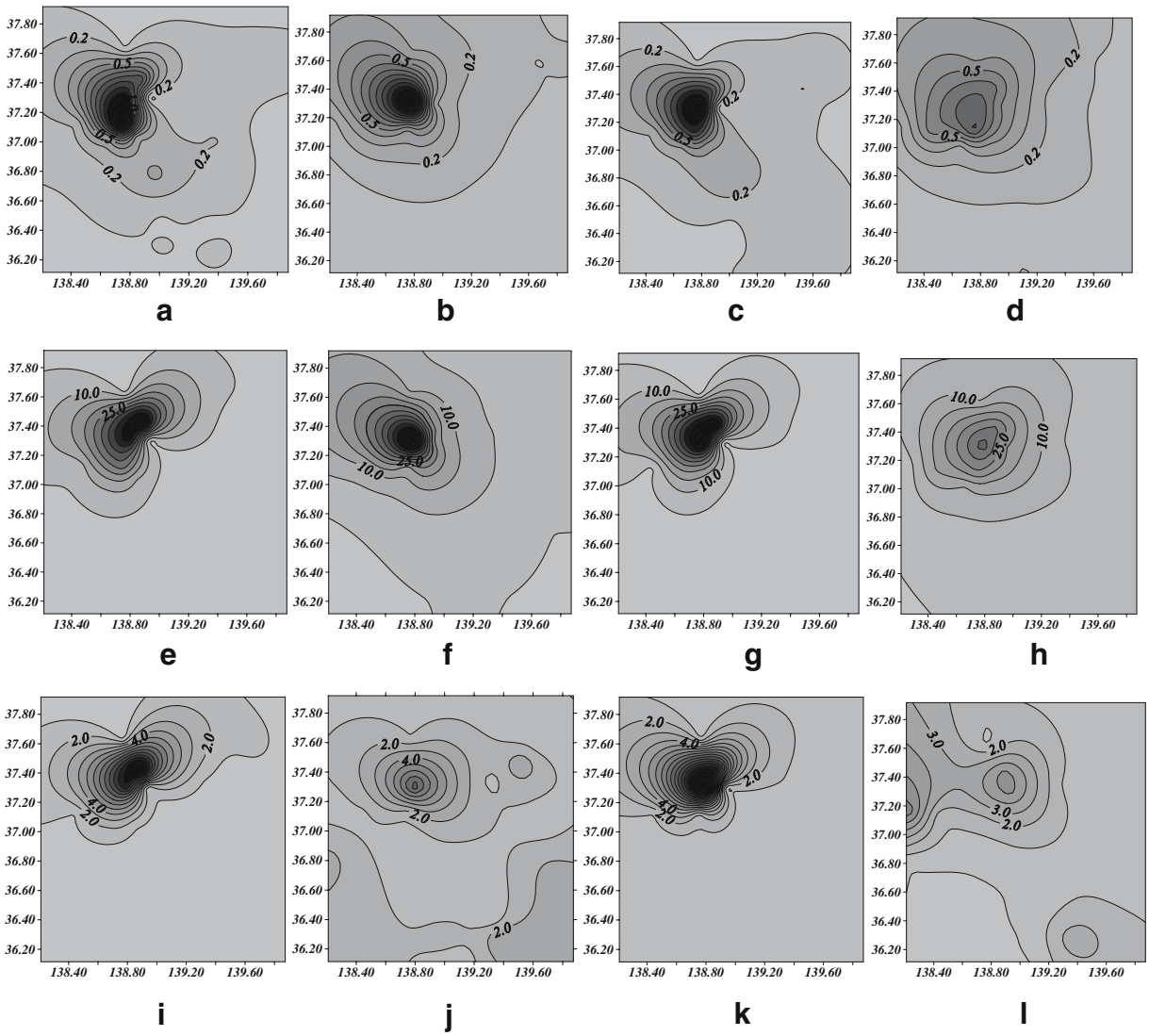

Fig. 7 Contours of peak ground acceleration (in the % of **g**) from Observed (**a**), simulated of NS component (**b**), observed EW (**c**) and simulated EW (**d**) components. Contours of peak ground velocity (in cm/s) from observed (**e**), simulated of NS component (**f**), observed EW (**g**) and simulated EW components (**h**) Contours of peak ground displacement (in cm) from observed (**i**), simulated of NS (**j**) component, observed EW (**k**) and simulated EW component (**l**)

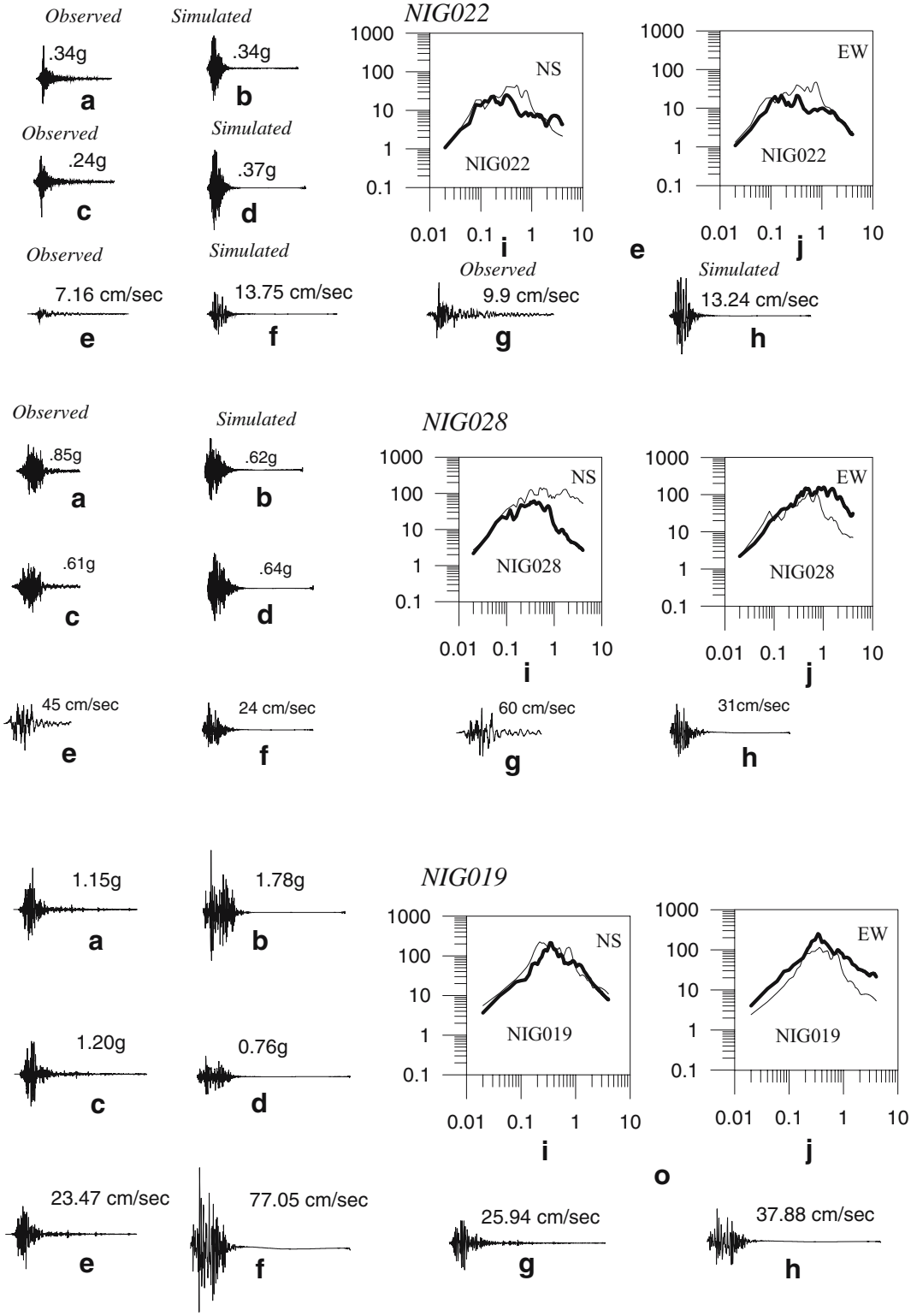
Observed
Simulated
.34g
a
.34g
b
Observed
Simulated
.24g
c
.37g
d
Observed
Simulated
7.16 cm/sec
e
13.75 cm/sec
f
NIG022
1000
100
10
1
0.1
NS
NIG022
0.01 0.1 1 10
i
EW
NIG022
j
Observed
9.9 cm/sec
g
Simulated
13.24 cm/sec
h
Observed
Simulated
.85g
a
.62g
b
.61g
c
.64g
d
45 cm/sec
e
24 cm/sec
f
NIG028
NS
NIG028
i
EW
NIG028
j
60 cm/sec
g
31cm/sec
h
1.15g
a
1.78g
b
1.20g
c
0.76g
d
23.47 cm/sec
e
77.05 cm/sec
f
NIG019
NS
NIG019
i
EW
NIG019
j
o
25.94 cm/sec
g
37.88 cm/sec
h

◀**Fig. 8** **a** Observed and **b** simulated NS; **c** observed and **d** simulated EW component of acceleration record. **e** Observed and **f** simulated NS; **g** observed and **h** simulated EW component of velocity record. Comparison of response spectra prepared from NS (**i**) and EW (**j**) components of observed and simulated records at NIG022, NIG028 and NIG019 stations. The station names are shown inside the figure showing response spectra. The response spectra shown by *thick black line* represent that prepared from observed record

follow a sinistral fault segment, which starts from Yuno valley and extends to Kashiwazaki. The strikes of the known faults, which have a main trend of NE–SW, are similar to the folding axes.

The maximum peak ground acceleration of 818 gal is recorded at Nagaoka station (Fig. 2) of KiK-NET, and the maximum peak ground acceleration of 1,715 gal has been recorded at Tohkamachi station (Fig. 2) of K-NET. The nearest station that has recorded this earthquake is Ojiya (Fig 2), which lies at an epicentral distance of 10 km, and it has recorded peak ground acceleration of 1,307 gal. This earthquake was also recorded on a broadband seismograph network installed under project "FREESIA" (F-net) by NIED, Japan. Mechanism of this earthquake is given by F-net site using the data observed by its network. The focal mechanism of the main shock shows a reverse fault with a compression axis in a NW–SE direction. The direction of the estimated fault follows the aftershock distribution.

The observed seismic intensity during the 2004 Niigata-ken Chuetsu earthquake was VII recorded by Japan Meteorological Agency JMA at Kawaguchi town. It brought catastrophic damage in the vicinity of North Uonuma and South Higashiyama hills. The overall population of the earthquake-affected region is about 300,000 (Aydan 2004). The main cities in the region are Nagaoka and Ojiya. The other large towns affected by the earthquake are Kawaguchi, Tohkamachi, Koide, Mitsuke and Muikamachi. The heavy damage due to the many slope failures induced by the earthquake was observed in Yamakoshi village with a population of 2,000. The most severely damaged town is Kawaguchi, which has a population of 5,500.

In the present simulation, the modelling parameters of the 2004 Niigata-ken Chuetsu earthquake are kept similar to that assumed by Honda et al. (2004) for the estimation of source parameters of this earthquake. These earthquake parameters are given in Table 5. The projection of the rupture plane is shown in Fig. 2. To have simulations at different locations, we have selected 23 stations surrounding the rupture plane. The site amplification at each station is computed from the records of past events recorded at same station.

The rupture plane is placed at a depth of 13 km from surface of earth in a layered velocity model shown in Table 4. This rupture plane is divided into 12 subfaults. Following the scaling relationship suggested by Sato (1989), each subfault corresponds to an earthquake of magnitude 4.9. Using the technique presented in this paper, NS and EW horizontal components of accelerogram due to target earthquake at 23 stations are simulated. Standard signal processing tools have been used to compute the velocity, displacement and response spectra from observed and simulated acceleration records. Parameters like peak ground acceleration, velocity and displacement have been computed from simulated and observed records for comparison.

Contour maps of acceleration, velocity and displacement have been prepared from both observed and simulated records and are shown in Fig. 7. It is seen from Fig. 7 that the general trend of distribution of peak ground acceleration from simulated records matches closely with that from observed records in the near field region. A good match is seen in the trend at far field station in EW component (Fig. 7c and d). Similar match in the distribution of peak ground velocity and peak ground displacement is seen in the near field regions. The distribution of peak ground acceleration, peak ground velocity and displacement at far field stations prepared from simulated records is less than in observed records. This is particularly due to the fact that in this approach, we are modelling accelerograms due to S waves only, and at near field distances, maximum contribution to ground motion can be caused by S-wave phases. In addition, at far field stations, other factors like local heterogeneities and tectonics also play equal role in shaping maximum ground motion. Among simulations at 23 stations, Figs. 8 and 9 present the result of simulation at six stations. Station-wise comparison of simulated and observed strong ground motion at these stations is given as follows:

6.1 Shibukawa (NIG022)

This station lies at an epicentral distance of 31 km. The peak ground acceleration and peak velocity computed from simulated and observed records at this station

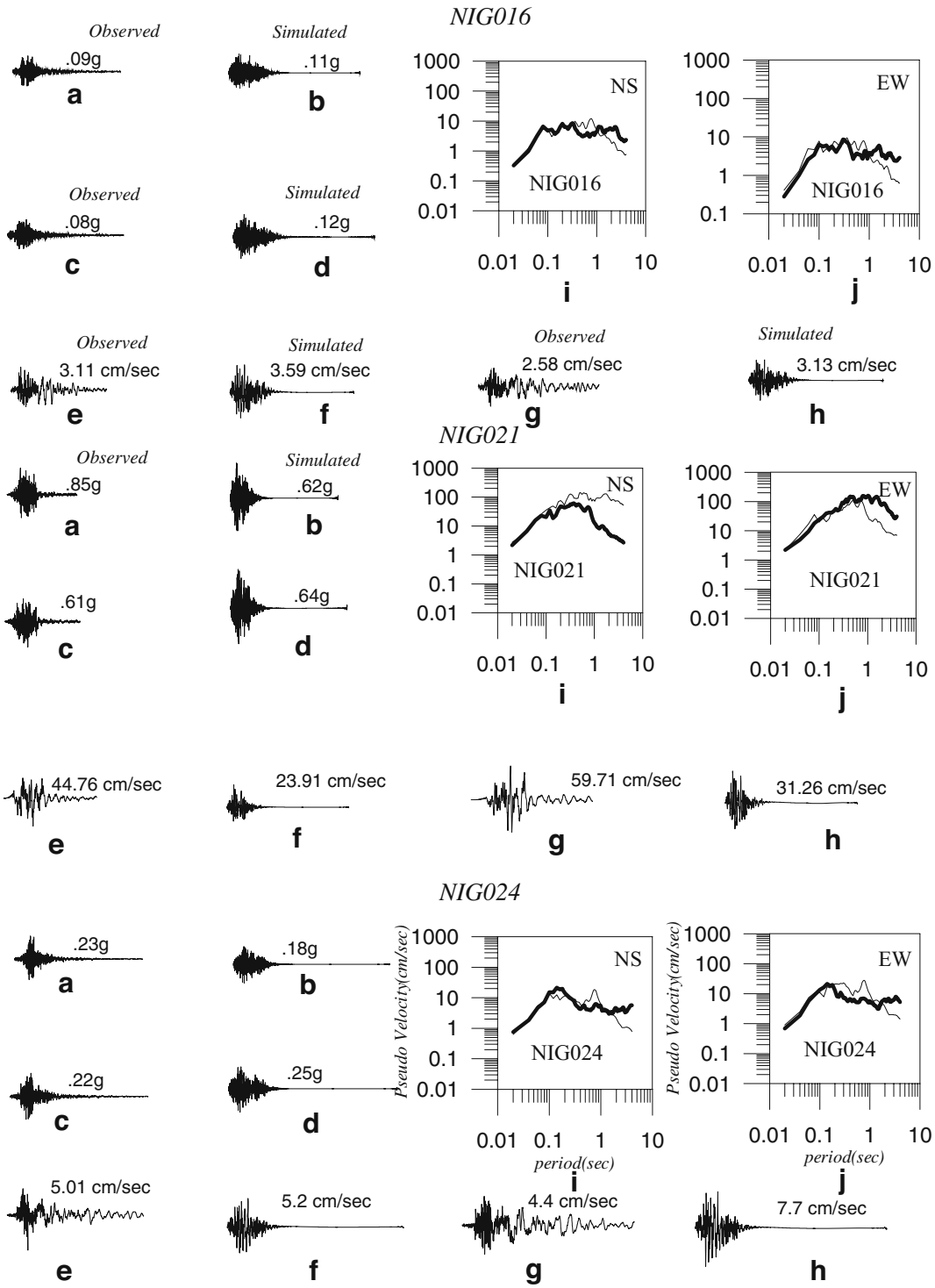

Fig. 9 **a**, **b**, **c**, **d**, **e**, **f**, **g**, **h**, **i** and **j** are same as mentioned in Fig. 8, but for stations NIG016, NIG021 and NIG024

shows close match. The duration of simulated and observed acceleration and velocity records also matches closely. The predominant period of NS and EW components also matches effectively, and comparable match is seen in both low and high frequencies.

6.2 Nagaoka-Shisho (NIG028)

This station lies at an epicentral distance of 15 km. The simulated records at this station has considerably low peak ground acceleration; however, comparable match in response spectrum is seen at high frequencies. This indicates that there is underestimation of site amplification at low frequencies, which may be due to presence of local heterogeneities.

6.3 Ojiya (NIG019)

This station lies at an epicentral distance of 10 km and is among the station very close to the epicenter of the 2004 Niigata-ken Chuetsu earthquake. The peak ground acceleration and peak ground velocity effectively match at this station. A good match is seen in the duration of simulated and observed velocity and acceleration waveform. The response spectrum from simulated and observed records at this station also matches effectively.

6.4 Teradomari (NIG016)

This station lies at an epicentral distance of 40 km. The peak ground acceleration and peak ground velocity from simulated and observed records at this station match closely. A good match in the duration of observed and simulated acceleration and velocity records is visible at this station. The response spectra also show good match in high frequencies, although some discrepancies at low frequencies are visible which may be due to local heterogeneities.

6.5 Tohkamachi (NIG021)

This station is lies at an epicentral distance of 24 km. At this station, the simulated acceleration and velocity records give less peak ground acceleration and peak ground velocity values. The clear match in the response spectra is seen at high frequencies; however, some discrepancies are observed at low frequencies, which may be accounted due to local heterogeneities.

6.6 Yasuduka (NIG024)

This station lies at an epicentral distance of 45 km and falls in the direction of rupture propagation. Although Teradomari (NIG016) station also lies at same epicentral distance, it has recorded less peak ground acceleration and peak ground velocity as compared to this station, which is due to the directivity effect. At this station, peak ground acceleration and peak ground velocity from simulated record match closely with the observed record. Considerable and good match is seen in the response spectra at high frequencies.

The station-wise comparison shows that this technique is capable of simulating strong ground motion at near field as well as far field stations in a frequency range 1–50 Hz. Mismatch at many stations are evident at frequencies less than 1.0 Hz. In most of the cases, contribution of simulated record is less in this low-frequency range. This may be due to local heterogeneities present beneath the stations. Further, the isoacceleration contours prepared from field and observed data show that at distances more than 110 km, some high isoacceleration contours are observed in field data which are absent in the isoacceleration contours prepared from simulated data. This is mainly because at far field distances, the high frequency contribution in strong motion records are attenuated due to earth medium acting as a high cut filter. At these stations, low-frequency contribution in strong motion record also contributes significantly to peak ground acceleration which does not match well with the field record. This result is due to local heterogeneities which are present in actual earth case. The present method is strongly dependent on scaling laws which are empirical in nature. Therefore, the successful prediction of strong ground motion parameters is entirely dependent on applicability of scaling laws in the region. Although the method of H/V ratio can be used for conversion of vertical component into horizontal components, it still lacks the representation of radiation pattern.

7 Conclusions

This paper presents a simplified hybrid method for the simulation of strong ground motion. The acceleration envelope function from each subfault is multiplied with the filtered white Gaussian noise having fre-

quency characteristics of strong ground motion. The correction function for the slip distribution of the large and small earthquakes and the transmission of energy at each layer is incorporated in the technique to simulate the synthetic accelerogram. These synthetic accelerograms are used as the Green's function in the EGF technique of Irikura (1986). Using the obtained site amplification curves at various sites, NS and EW components of strong ground motion are simulated. As a case study, simulations are made for the 2004 Niigata-ken Chuetsu, Japan earthquake at numbers of stations. The parameters of synthetic strong motion records and their comparison establish the efficacy of the approach to model earthquake using simple regression relations and parameters not so difficult to estimate. The comparison shows that this technique is capable of simulating strong motion records with realistic appearance and properties, which matches well with actual records.

Acknowledgements Authors sincerely acknowledge the data collected by Kyoshin network maintained by NIED, Japan. The work presented in this paper is outcome of DST project no. DST/23 (483) /SU/2004.

References

Abrahamson NA, Litehiser JJ (1989) Attenuation of vertical peak acceleration. Bull Seismol Soc Am 79:549–580

Aydan Ö (2004) A reconnaissance report on Niigata-ken Chuetsu earthquake of October 23, 2004. Department of Marine Civil Engineering, Shizuoka, Japan

Bardet JP (2004) Preliminary observations of the Niigata-ken Chuetsu, Japan, earthquake of October 23, 2004. A preliminary report for the EERI-GEER Earthquake Engineering Reconnaissance Team

Beresnev IA, Atkinson GM (1997) Modelling finite fault radiation from ω^n spectrum. Bull Seismol Soc Am 87:67–84

Boore DM (1983) Stochastic simulation of high frequency ground motion based on seismological models of radiated spectra. Bull Seismol Soc Am 73:1865–1894

Boore DM, Atkinson CM (1987) Stochastic prediction of ground motion and spectral response parameters at hard rock sites in eastern North America. Bull Seismol Soc Am 77:440–467

Brune JN (1970) Tectonic stress and spectra of seismic shear waves from earthquakes. J Geophys Res 76:5002

Hadley DM, Helmberger DV (1980) Simulation of strong ground motions. Bull Seismol Soc Am 70:617–610

Hartzell SH (1978) Earthquake aftershocks as Green functions. Geophys Res Lett 5:1–4

Hartzell SH (1982) Simulation of ground accelerations for May 1980 Mammoth Lakes, California earthquakes. Bull Seismol Soc Am 72:2381–2387

Honda R, Aoi S, Sekiguchi H, Morikawa N, Kunugi T, Fujiwara H (2004) Ground motion and rupture process of the 2004 mid Niigata Prefecture earthquake obtained from strong motion data of K-NET and KiK-net (from website http://www.k-net.bosai.go.jp/k-net)

Horike M, Zhao B, Kawase H (2001) Comparison of site response characteristics inferred from microtremors and earthquake shear waves. Bull Seismol Soc Am 91:1526–1536

Hutchings L (1985) Modelling earthquakes with empirical Green's functions (abs). Earthq Notes 56:14

Irikura K (1983) Semi empirical estimation of strong ground motion during large earthquakes. Bulletin of Disaster Prevention Research Institute (Kyoto Univ.) 33:63–104

Irikura K (1986) Prediction of strong acceleration motion using empirical Green's function. Proceed. 7th Japan Earthquake Engineering Symposium, pp 151–156

Irikura K, Muramatu I (1982) Synthesis of strong ground motions from large earthquakes using observed seismograms of small events. Proceedings of the 3rd International Microzonation Conference, Seattle, pp 447–458

Irikura K, Kagawa T, Sekiguchi H (1997) Revision of the empirical Green's function method by Irikura, 1986, Programme and Abstracts. The Seismological Society of Japan 2:B25

Joshi A (1997) Modelling of peak ground acceleration for Uttarkashi earthquake of 20th October 1991. Bull Indian Soc Earthq Technol 34:75–96

Joshi A (2004) A simplified technique for simulating wide band strong ground motion for two recent Himalayan earthquakes. Pure Appl Geophys (PAGEOPH) 8:161

Joshi A, Midorikawa S (2004) A simplified method for simulation of strong ground motion using rupture model of the earthquake source. J Seismol 8:467–484

Joshi A, Midorikawa S (2005) Attenuation characteristics of ground motion intensity from earthquakes with intermediate depth. J Seismol 9:23–37

Joshi A, Singh S, Kavita G (2001) The simulation of ground motions using envelope summations. Pure Appl Geophys 158:877–901

Kamae K, Irikura K (1992) Prediction of site specific strong ground motion using semi-empirical methods. Proceedings of the 10th World Conference on Earthquake Engineering, pp 801–806

Kamae K, Irikura K (1998) Source model of the 1995 Hyogo-ken Nanbu earthquake and simulation of near source ground motion. Bull Seismol Soc Am 88:400–412

Kanamori H (1979) A semi empirical approach to prediction of long period ground motions from great earthquakes. Bull Seismol Soc Am 69:1645–1670

Kanamori H, Anderson DL (1975) Theoretical basis of some empirical relations in seismology. Bull Seismol Soc Am 65:1073–1095

Kiyono J (1992) Identification and synthesis of seismic ground motion in structural response analysis. Ph. D. thesis, Department of Civil Engineering Kyoto University

Lai SP (1982) Statistical characterization of strong ground motions using power spectral density function. Bull Seismol Soc Am 72:259–274

Lee WHK, Stewart SW (1981) Principles and applications of microearthquake networks. Academic, New York, p 293

Midorikawa S (1993) Semi empirical estimation of peak ground acceleration from large earthquakes. Tectonophysics 218:287–295

Mikumo T, Irikura K, Imagawa K (1981) Near field strong motion synthesis from foreshock and aftershock records and rupture process of the main shock fault (abs.). IASPEI 21st General Assembly, London

Mugnuia L, Brune JM (1984) Simulations of strong ground motions for earthquakes in the Mexicali-Imperial Valley. Proceedings of Workshop on Strong Ground Motion Simulation and Earthquake Engineering Applications, Pub. 85-02 Earthquake Engineering Research Institute, Los Altos, California, 21-1-21-19

Nakamura Y (1988) Inference of seismic response of surficial layer based on microtremor measurement. Quaterly report on railroad research 4. Railway Technical Railway Institute, pp 18–27 (in Japanese)

Saikia CK (1993) Ground motion studies in great Los Angles due to M_w=7.0 Earthquake on the Elysian Thrust Fault. Bull Seismol Soc Am 83:780–810

Saikia CK, Herrmann RB (1985) Application of waveform modelling to determine focal mechanisms of four 1982 Miramichi aftershocks. Bull Seismol Soc Am 75:1021–1040

Sato R (1989) Handbook of fault parameters of Japanese earthquakes Kajima, Tokyo, 390 pp (in Japanese)

Sato HP, Abe K, Otaki O (2001) GPS-measured land subsidence in Ojiya City, Niigata Prefecture. Jpn Eng Geol 60:379–390

Seo K, Samano T (1993) Use of microtremor for prediction of seismic motion. Report of General Research (A) under contract with the ministry of education, pp 198–200 (in Japanese)

Somerville P, Irikura K, Graves R, Sawada S, Wald D, Abrahamson N, Iwasaki Y, Kagawa T, Smith N, Kowada A (1999) Characterising crustal earthquake slip models for the prediction of strong ground motion. Seismol Res Lett 70(1):59–80

Yu G (1994) Some aspect of earthquake seismology: slip partitioning along major convergent plate boundaries; composite source model for estimation of strong motion; and nonlinear soil response modelling. Ph.D. thesis, University of Nevada, Reno

Yu G, Khattri KN, Anderson JG, Brune JN, Zeng Y (1995) Strong ground motion from the Uttarkashi earthquake, Himalaya, India, earthquake: comparison of observations with synthetics using the composite source model. Bull Seismol Soc Am 85:31–50

Zeng Y, Anderson JG, Su F (1994) A composite source model for computing realistic synthetic strong ground motions. Geophys Res Lett 21:725–728